A Reconfigurable Dual Resonant Inverter with Independent Control for Induction Heating

Ramesh Junju
Department of Electrical Engineering
National Institute of Technology Warangal
Warangal, India
rj721031@student.nitw.ac.in

S. Porpandiselvi
Department of Electrical Engineering
National Institute of Technology Warangal
Warangal, India
selvi@nitw.ac.in

2024 IEEE 4th International Conference on Sustainable Energy and Future Electric Transportation (SEFET) | 979-8-3503-8399-7/24/$31.00 ©2024 IEEE | DOI: 10.1109/SEFET61574.2024.10718236

***Abstract*—The demand for flexible and adaptive power electronics solutions in industrial as well as domestic applications, particularly in Induction Heating (IH) with varying material properties necessitate tailored power delivery mechanisms. Conventional inverters typically operate in either full-bridge (FB) or in half-bridge (HB), limiting their adaptability and efficient operation when dealing with diverse loads. Different material compatibility is a desirable feature of the IH system. This paper presents a reconfigurable inverter tailored for IH applications. The proposed inverter exhibits the capability to dynamically switch between FB and HB configurations, offering enhanced versatility and efficiency in powering both ferromagnetic (FM) and non-ferromagnetic (NFM) material loads. The reconfigurable inverter's dual frequency operation enables independent control of two different material loads. The proposed inverter operates in HB mode to power FM load at low-frequency and in FB mode to power NFM load at high-frequency. Asymmetrical Duty Cycle (ADC) control is used in HB mode and Asymmetrical Voltage Cancellation (AVC) control is used in FB mode. Soft switching is accomplished to provide a greater output power range. The proposed inverter topology has been verified through MATLAB simulation for an output power of 1.7 kW and an efficiency of 95.7% is achieved.**

Keywords*— *Asymmetrical Duty Cycle Control, Asymmetrical Voltage Cancellation Control, Induction Heating, Reconfigurable inverter, Series resonant inverter, and Zero Voltage Switching (ZVS).

I. Introduction

Induction heating (IH) is a process that uses electromagnetic induction to heat electrically conductive materials. The principle behind IH involves generating high-frequency alternating currents in a coil, which produces a rapidly alternating magnetic field. When a conductive material is placed within this magnetic field, emf is induced within the material, generating eddy currents which produces heat due to its electrical resistance. IH has emerged as an efficient method and versatile for heating metallic objects in domestic applications [1]. Compared to traditional heating techniques, IH has a number of benefits that make it a better option for domestic applications. Efficiency, cleanliness, quick heating, accurate control, adaptability, consistent heating, and safety are some of IH's main benefits [2]. In IH, the skin depth plays a crucial role in determining the depth of penetration of the alternating magnetic field into the material being heated. The relation between switching frequency and skin depth is given in (1).

$$\delta = \sqrt{\frac{\rho}{\pi \mu f}} \tag{1}$$

where ρ is the resistivity of the material, f is the frequency of the current, and μ is the magnetic permeability of the material.

The efficiency with which series resonant inverters (SRI) can provide the high-frequency alternating currents required to heat the workpiece makes them a popular choice for IH applications. Some commonly used SRIs in induction heating are full-bridge [3], half-bridge [4], and single-switch [5] topologies. Power for a single heating element or cooking zone is supplied via a single-load SRI arrangement. For residential induction cooktops with a single cooking zone, the single-load SRI setup is appropriate due to its affordability and simplicity. Nevertheless, it might not be adaptable enough to support several cooking zones at a time. As a result, multi-load configurations are now being developed in SRIs. Some resonant tank circuits are used in a multi-load SRI arrangement to supply several heating elements simultaneously and independently.

Multi-load SRI setup enables the simultaneous heating of numerous loads made of various materials, such as FM and NFM materials, at various power levels. When exposed to the alternating magnetic fields produced by the inverter, these FM and NFM materials behave differently. For FM materials, the admittance is high at lower switching frequencies. For NFM materials, on the other hand, the admittance is large at higher switching frequencies.

In order to manage the temperature of the workpiece and adjust the output power, power control techniques are crucial. Pulse frequency modulation (PFM) [6], asymmetrical duty cycle (ADC) control [7], phase shift control (PS), and asymmetrical voltage cancellation (AVC) control [8] are few of the power control strategies frequently used in SRIs.

Reconfigurable resonant inverters have a number of benefits, including increased efficiency, flexibility, and adaptability. A reconfigurable inverter with series and series-parallel resonant loads is proposed in [9] for induction heating. It uses additional components such as electromechanical switch, an inductor, and a capacitor, which increases the system's overall size, weight, and cost.

In this paper, a reconfigurable resonant inverter is proposed to power two different material IH loads i.e., aluminum (NFM) and iron (FM) loads operating in FB and HB modes respectively. During high state of the control pulse, the inverter configures to FB mode and powers the aluminum load. And during the low state of the control pulse, the inverter configures to HB mode and powers the iron load. ADC control is used to control the power in iron load and AVC control is used to control the power in aluminum load.

This paper is organized as follows: The proposed reconfigurable resonant inverter is presented in Section II.

The inverter output power and its control are described in Section III. In Section IV, the operating modes of the reconfigurable inverter are presented. Section V presents the simulation results to validate the proposed inverter's feasibility. Finally, Section V concludes the paper.

II. Circuit Description and its Operation

Circuit diagram of the proposed resonant inverter is shown in Fig. 1. A DC voltage source, V_S, and four MOSFET switching devices, M_A to M_D, form a full-bridge circuit. Load-1 is treated as a NFM load and R_{eq_1} and L_{eq_1} represent the load-1 equivalent resistance and inductance, respectively. The resonant capacitor C_{r_1} is employed in order to resonate the load-1. Load-2 is treated as a FM load and its equivalent resistance and equivalent inductance are represented by R_{eq_2} and L_{eq_2} respectively. C_{r_2} serves as the load-2 resonant capacitor.

The load-1 is powered by high switching frequency of f_H as the NFM material has high admittance at higher frequencies. Whereas the load-2 is powered by a low switching frequency (f_L) since the FM material has high admittance at lower frequencies. The MOSFETS M_C and M_D remain always in the OFF and ON positions, respectively, during the FM load's powering period (t_2) and MOSFETS M_A and M_B are switched at a frequency of f_L. The circuit operates as a half-bridge inverter in this mode.

The proposed inverter can be reconfigured to operate both in HB and FB modes to power load-2 and load-1 with low and high frequencies respectively. This reconfiguration operation is governed by a control pulse, G_C. When the state of G_C is high, high-frequency pulses are generated and the inverter operates in full-bridge mode. When the state of G_C is low, low-frequency pulses are generated and the inverter operates in half-bridge mode. Fig. 2 shows the gating pulses of the switching devices.

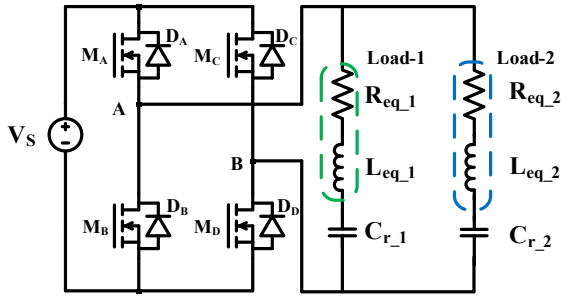

Fig. 1. Proposed Reconfigurable Resonant Inverter.

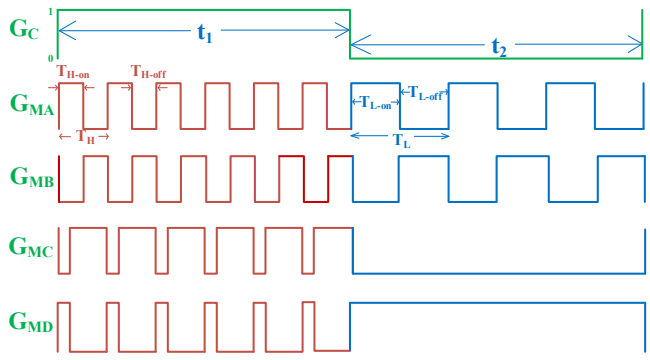

Fig. 2. Switching pulses.

However, in order to supply the load-1, all MOSFETS from M_A to M_D are switched at a frequency of f_H during t_1. M_A and M_B are operated complementary. In a similar way, M_C and M_D are complement to each other. There is sufficient dead time in between each leg's switching to keep the inverter from sustaining a shoot-through current. The circuit operates as a full-bridge inverter during this mode.

$T_{H\text{-}on}$, $T_{H\text{-}off}$, and T_H are respectively the ON period, OFF period, and total time period of the high-frequency pulse. Similarly, $T_{L\text{-}on}$, $T_{L\text{-}off}$, and T_L are the ON period, OFF period, and total time period of the low-frequency pulse respectively. T_L and T_H are expressed in (2). The duration of the control pulse during its high and low states are denoted by t_1 and t_2 respectively. Thus, the powering period of the particular load can be controlled by varying t_1 and t_2 of G_C. If the FM load is to be powered alone, then t_1 of G_C is set to minimum. In contrast, if the NFM load is to be powered alone, then t_2 of G_C is set to minimum.

$$T_L = \frac{1}{f_L}, \quad T_H = \frac{1}{f_H} \tag{2}$$

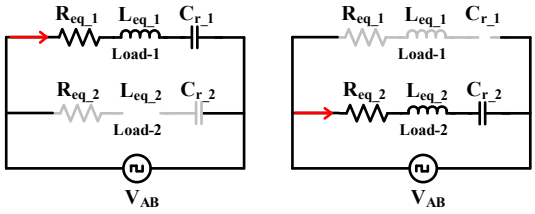

(a) during t_1 (b) during t_2

Fig. 3. Resonant load operation.

Load-1 resonant frequency is expressed as $f_{r1} = \frac{1}{2\pi\sqrt{L_{eq\_1}C_{r\_1}}}$. During t_1, the inverter is operated at a high frequency of 220 kHz in FB mode. The $\frac{f_H}{f_{r1}}$ ratio is selected to be 1.02 in order to make the circuit slightly lagging which facilitates ZVS.

Load-2 resonant frequency is expressed as $f_{r2} = \frac{1}{2\pi\sqrt{L_{eq\_2}C_{r\_2}}}$. During t_2, the inverter is operated at a low frequency of 30 kHz in HB mode. The $\frac{f_L}{f_{r2}}$ ratio is selected to be 1.1 in order to make the circuit slightly lagging which facilitates ZVS.

During t_1 and t_2 the equivalent circuit of the resonant loads are shown in Fig. 3. During t_1 the inverter is operated at f_H which is closer to the resonant frequency of load-1. Load-1 offers low impedance path for high frequency currents. Whereas in load-2, L_{eq_2} offers a high impedance at f_H and hence acts as an open circuit. Hence the entire high frequency inverter current flows through load-1 only.

On the other hand, during t_2 the inverter is operated at f_L which is closer to the resonant frequency of load-2. Load-2 offers low impedance path for low frequency currents. Whereas in load-1, C_{r_1} offers a high impedance at f_L and hence acts as an open circuit. Hence the entire low frequency inverter current flows through load-2 only.

III. Output Power and Its Control

The equivalent circuit during FB and HB operating modes of the proposed inverter are shown in Fig. 4. The inverter configures to FB mode to power load-1 and to HB mode when powering load-2. AVC technique is used to control the power of load-1 in FB mode and ADC technique is used to control the power of load-2 in HB mode. To reduce the switching losses, the inverter is operated slightly above the respective resonant frequencies of the loads by facilitating Zero Voltage Switching (ZVS).

Load-1 is powered for a time duration of t_1, while load-2 is powered for a time duration of t_2.

Let the maximum power rating of both loads be P_{Max}.

The average power of load-1 can be expressed as

$$P_1 = \frac{t_1}{(t_1+t_2)} P_{Max} \quad (3)$$

and the average power of load-2 is

$$P_2 = \frac{t_2}{(t_1+t_2)} P_{Max} \quad (4)$$

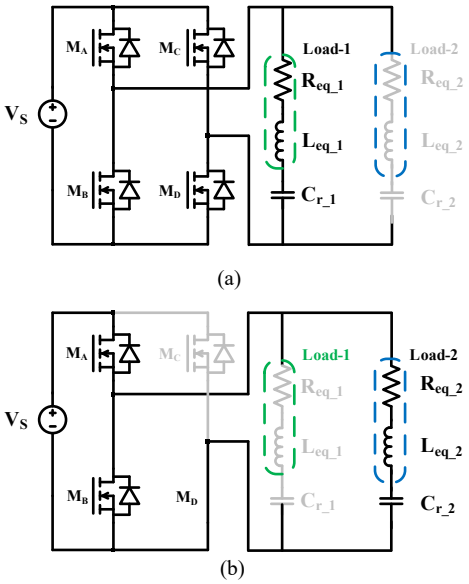

Fig. 4. Equivalent circuit of the inverter: (a) FB mode (b) HB mode

The total average power is $P_1 + P_2 = P_{Max}$

If $P_1 = P_2 = P_L(say)$, then $P_L = 0.5P_{Max}$

The time duration for powering the load-1,

$$t_1 = \frac{P_1 T}{P_{Max}} \quad (5)$$

The time duration for powering load-2,

$$t_2 = \frac{P_2 T}{P_{Max}} \quad (6)$$

where, $T = t_1+t_2$, is the time period of the control signal.

Load-1 alone can be powered by making t_2 as zero and load-2 alone can be powered by making t_1 as zero. Thus, the time durations t_1 and t_2 determine the powering period of the loads.

IV. Modes of Operation

The detailed operating principle of the inverter operating in FB and HB modes is presented below.

A. Operating principle of FB-mode:

The major modes of operation of the inverter in FB-mode are shown in Fig. 5. During this operation, all the switching devices M_A to M_D are switched at high frequency, f_H, during the high state of the control pulse G_C and powers load-1.

1) FB mode-1: In this mode of operation, switching devices M_A and M_D are in on state, powering load-1. The voltage across the inverter terminals A and B is $+V_S$.

2) FB mode-2: During this mode, M_A and M_C are in on state, therefore the load-1 current freewheels and hence the inverter output voltage is zero.

3) FB mode-3: In this final mode of operation, the switching devices M_B and M_C are ON and hence $V_{AB} = -V_S$.

The corresponding output voltage waveform during t_1 is shown in Fig. 7.

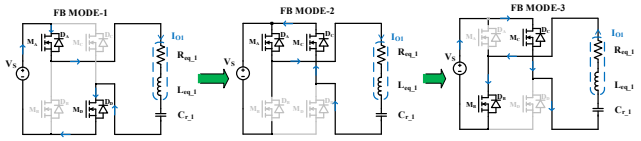

Fig. 5. FB mode: Modes of operation

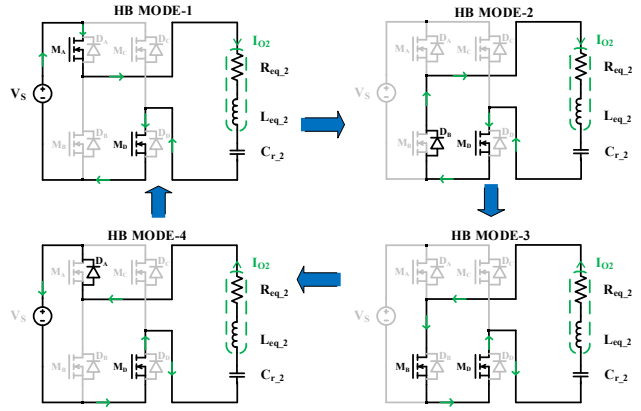

Fig. 6. HB mode: Modes of operation

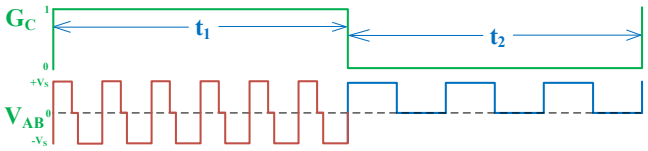

Fig. 7. Control pulse G_C and inverter output voltage, V_{AB}.

B. Operating principle of HB-mode:

The modes of operation of the inverter in HB-mode are shown in Fig. 6. In this mode of operation, the switching devices M_C and M_D are in off and on states respectively. Switching devices M_A and M_B are switched at low frequency, f_L, and powers load-2.

1) HB mode-1: During HB mode-1, M_A and M_D are ON, hence $V_{AB} = V_S$.

2) HB mode-2: In HB mode-2, M_A turns off and M_B is about to turn on during the dead time period. As the load-2 is operated to be more inductive in nature, load-2 current

freewheels through D_B and hence $V_{AB} = 0$. This ensures the ZVS of M_B.

3) HB mode-3: During HB mode-3, M_B is ON, load is disconnected from the supply and therefore, $V_{AB} = 0$.

4) HB mode-4: In HB mode-4, M_B turns off, M_A is about to turn on and load current freewheels through D_A and hence, $V_{AB} = V_S$.

The corresponding output voltage waveform during t_2 is shown in Fig. 7.

V. Simulation Results and Analysis

The MATLAB® environment is utilized for the design and simulation of the proposed reconfigurable inverter. The maximum output power of the inverter, when each load is powered at 850 watts, is 1.7 kW. Table I provides the design specifications.

An aluminum vessel is treated as the load-1 which is a NFM load and an iron pan is treated as the load-2 which is a FM load. FM load is driven by configuring the inverter in half-bridge mode whereas the NFM load is driven by configuring the inverter in full-bridge mode. For inverter operation mode control, a control pulse G_C of frequency 20 Hz is selected. To power load-1, the switching frequency, f_H is selected, and to power load-2, a switching frequency, f_L is selected. The FFT of the inverter output current is displayed in Fig. 8. It indicates that the inverter is operating with dual frequency. It can be observed from Fig. 9, that the inverter reconfigures its mode of operation from a full bridge to a half-bridge and vice-versa during each 25 msec. The control pulse is high during 25 msec operating the inverter in full-bridge mode and it becomes low for 25 msec operating the inverter in half-bridge mode.

It can be observed from Fig. 10 that the load-2 is powered during the low state of G_C, configuring the inverter in HB mode and load-1 is powered during the high state of G_C, configuring the inverter in FB mode. A negligible amount of current flows through the loads during their respective non-powering period.

TABLE I. Circuit Parameters

Parameters	Value
DC Input Voltage, V_{DC}	110 V
Load-1 Switching Frequency, f_H	220 kHz
Load-2 Switching Frequency, f_L	30 kHz
Control Pulse frequency	20 Hz
Equivalent Resistance of both the loads, $R_{eq-L} = R_{eq-H}$	2.8 Ω
Equivalent Inductance of Load-1, L_{eq-1}	54.3 µH
Equivalent Inductance of Load-2, L_{eq-2}	65.8 µH
Resonant Capacitance of Load-1, C_{r-1}	10 nF
Resonant Capacitance of Load-2, C_{r-2}	0.52 µF

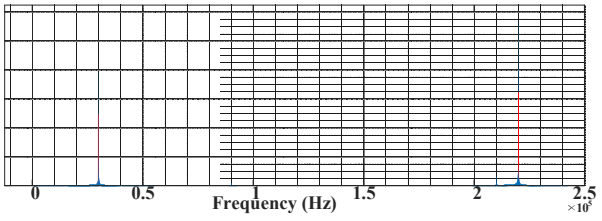

Fig. 8. FFT of the inverter output current

During FB mode, load-1 current is almost zero and is negligible. This can be observed in Fig. 11. Similarly, during HB mode, load-2 current is almost zero and is negligible. This can be observed in Fig. 12. Independent power control of load-1 varying the duty ratio of the inverter, D_1 during HB mode is shown in Fig. 11. During this independent control, the inverter is operated at 50% duty ratio in FB mode. Fig. 14 shows the independent power control of load-2, varying the ON period duty ratio of the inverter, D_2 during FB mode. During this independent control, the inverter is operated at 50% duty ratio in HB mode. Hence it is evident that the independent control of the two loads is possible in the proposed inverter. A peak power of 1.7 kW is delivered to the loads at the maximum duty ratio.

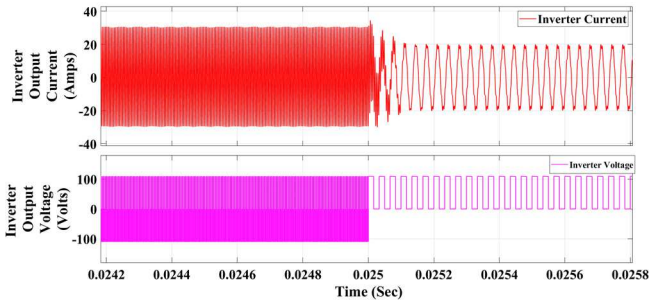

Fig. 9. Simulation waveforms: Inverter output current (Top) and Inverter output voltage (Bottom).

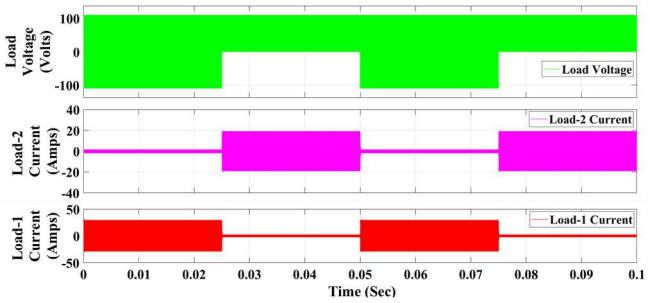

Fig. 10. Simulation waveforms: Load voltage (Top), load-2 current (Middle) and load-1 current (Bottom).

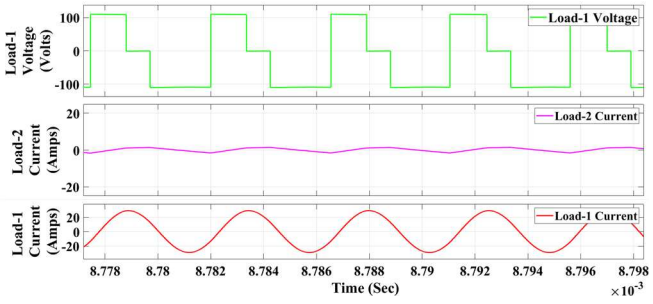

Fig. 11. Simulation waveforms during FB mode: Load-1 voltage (Top), load-2 current (Middle) and load-1 current (Bottom).

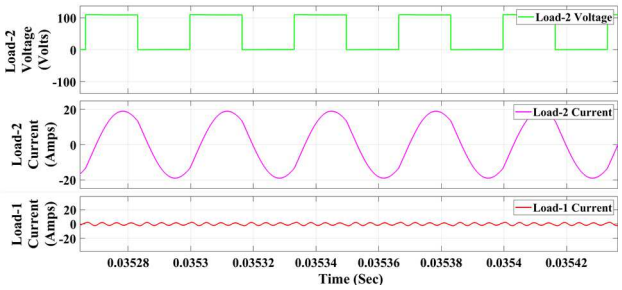

Fig. 12. Simulation waveforms during HB mode: Load-1 voltage (Top), load-1 current (Middle) and load-2 current (Bottom).

For the peak output power delivered, an efficiency of 95.7 % is obtained, and is depicted in Fig. 15.

Hence, the reconfigurable resonant inverter is versatile in powering two different types of material loads independently with high efficiency.

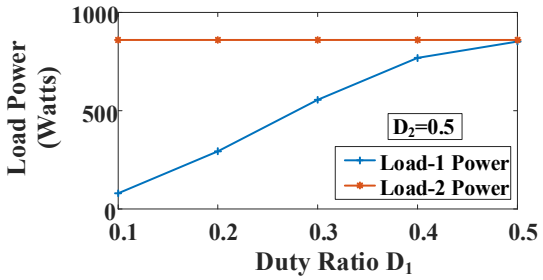

Fig. 13. Independent power control of Load-1.

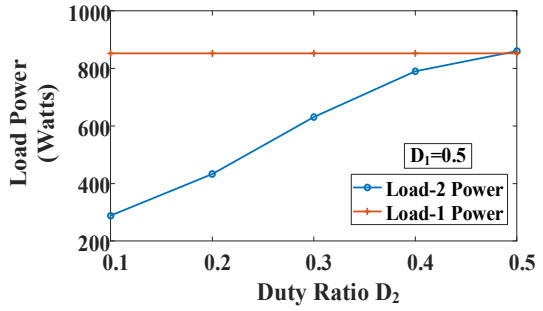

Fig. 14. Independent power control of Load-2.

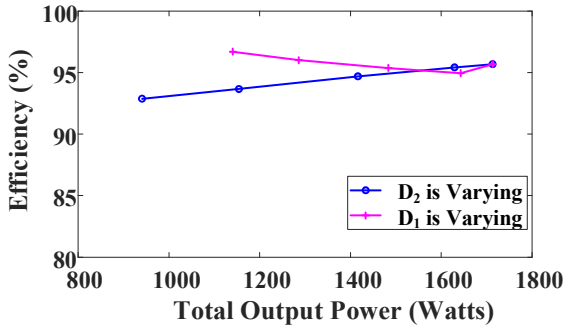

Fig. 15. Efficiency Vs Total output power.

VI. Conclusion

A dual resonant reconfigurable inverter for different material IH loads is proposed in this paper. A dual-resonant approach using dual frequency is used to power the load-1 and load-2. High frequency is used to power the load-1 in full-bridge mode and low frequency is used to power the load-2 in half-bridge mode. The independent power control of load-1 and load-2 is achieved using AVC and ADC respectively. The proposed inverter is simulated for 1.7 kW in MATLAB. The inverter operates at an efficiency of 95.7% and maintains a good efficiency profile in the entire range of power control of the loads. Hence, this dual resonant reconfigurable inverter is feasible for domestic induction cooking applications.

VII. References

[1] O. Lucía, P. Maussion, E. J. Dede and J. M. Burdío, "Induction Heating Technology and Its Applications: Past Developments, Current Technology, and Future Challenges," in IEEE Transactions on Industrial Electronics, vol. 61, no. 5, pp. 2509-2520, May 2014, doi: 10.1109/TIE.2013.2281162.

[2] Vishnuram P, Ramachandiran G, Ramasamy S, Dayalan S. A comprehensive overview of power converter topologies for induction heating applications. *Int Trans Electr Energ Syst*. 2020; 30:e12554. https://doi.org/10.1002/2050-7038.12554.

[3] S. Khatroth and P. Shunmugam, "Cascaded full-bridge resonant inverter configuration for different material vessel induction cooking," IET Power Electron., vol. 13, no. 19, pp. 4428–4438, 2020.

[4] B. Salvi, S. Porpandiselvi and N. Vishwanathan, "A Three Switch Resonant Inverter for Multiple Load Induction Heating Applications," in IEEE Transactions on Power Electronics, vol. 37, no. 10, pp. 12108-12117, Oct. 2022, doi: 10.1109/TPEL.2022.3173931.

[5] H. W. Koertzen, J. A. Ferreira, and J. D. van Wyk, "A comparative study of single switch induction heating converters using novel component effectivity concepts," in IEEE PESC, 1992, pp. 298–305.

[6] Khatroth S, Shunmugam P. Single-stage pulse frequency controlled AC–AC resonant converter for different material vessel induction cooking applications. *Int J Circ Theor Appl*. 2021; 49(9): 2865-2884. doi:10.1002/cta.3042.

[7] Ahmed T, Ogura K, Chandhaket S, Nakaoka M. Asymmetrical duty cycle controlled edge resonant soft switching high frequency inverter for consumer electromagnetic induction fluid heater. Autom ATKAAF. 2003;44(1-2):21-26.

[8] Burdio JM, Barragan LA, Monterde F, Navarro D, Acero J. Asymmetrical voltage-cancellation control for full-bridge series resonant inverters. IEEE Trans Power Electron. 2004;19(2):461-469.

[9] W. Han, K. T. Chau, W. Liu, X. Tian and H. Wang, "A Dual-Resonant Topology-Reconfigurable Inverter for All-Metal Induction Heating," in IEEE Journal of Emerging and Selected Topics in Power Electronics, vol. 10, no. 4, pp. 3818-3829, Aug. 2022, doi: 10.1109/JESTPE.2021.3071700.